Activation and Stabilization of Engineered Amine Dehydrogenase by Fatty Acids for Bioprocess Intensification of Asymmetric Reductive Amination

Kong, Weixi; Zhang, Jiawang; Zhou, Liya; Liu, Guanhua; He, Ying; Ma, Li; Hollmann, Frank; Wang, Lihui; Liu, Yunting; Jiang, Yanjun

DOI
10.1021/acscatal.4c05904

Publication date
2025

Document Version
Final published version

Published in
ACS Catalysis

ACS Catalysis

pubs.acs.org/acscatalysis Research Article

Activation and Stabilization of Engineered Amine Dehydrogenase by Fatty Acids for Bioprocess Intensification of Asymmetric Reductive Amination

Weixi Kong, Jiawang Zhang, Liya Zhou, Guanhua Liu, Ying He, Li Ma, Frank Hollmann, Lihui Wang, Yunting Liu,* and Yanjun Jiang*

Cite This: *ACS Catal.* 2025, 15, 34−43 Read Online

ACCESS | Metrics & More | Article Recommendations | Supporting Information

ABSTRACT: In this study, we present a significant advancement in the field of enzymatic asymmetric reductive amination (ARA) of ketones, a pivotal reaction for chiral amine synthesis. Through a combination of semirational enzyme design and bioprocess development, we achieve the dual activation and stabilization of amine dehydrogenase (AmDH) to meet industrial demands. The engineered AmDH exhibits remarkable catalytic efficiency (turnover number, TON >1,000,000) and exceptional stability (half-life >7 days at 50 °C), with a broadened substrate scope including various aryl alkyl ketones and fatty ketones. Leveraging biobased oleic acid as an activator and stabilizer, we achieved kilogram-scale synthesis of chiral amines. Furthermore, the integration of AmDH with chemical catalysts in chemoenzymatic cascades has enabled the synthesis of a wide array of pharmaceutically relevant amines from diverse substrates, demonstrating the enzyme's versatility and potential to transform synthetic chemistry.

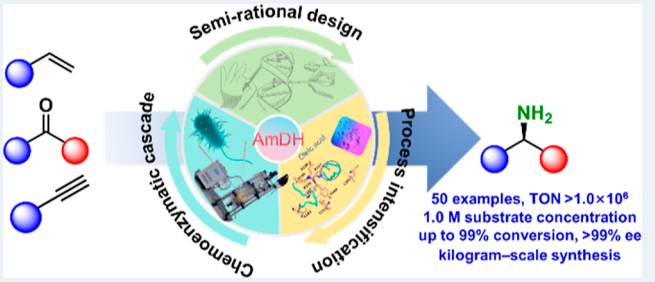

KEYWORDS: *amine dehydrogenase, bioprocess intensification, enzyme engineering, reductive amination, chiral amines*

INTRODUCTION

Chiral amines are omnipresent structural motifs and building blocks in pharmaceuticals, natural products, and bioactive molecules.[1,2] Consequently, it is not surprising that a diverse array of chemical synthetic strategies for chiral amines has been developed over the past decades, encompassing asymmetric hydrogenation of enamines and imines,[3,4] hydroalkylation of enamines,[5−7] *N*-alkylation of aliphatic amines,[8] amination of C−H bonds,[9,10] carbene insertion into N−H bonds of aliphatic amines,[11] hydroamination of alkenes,[12−14] and notably, the asymmetric reductive amination reaction (ARA) of prochiral ketones.[15−18] These chemical strategies, although effective, commonly require expensive transition metals and synthetically laborious chiral ligands, rendering commercial manufacturing ultimately costly and environmentally unsustainable.

Concurrently, enzymatic alternatives for chiral amine synthesis have rapidly evolved alongside these chemocatalytic methodologies.[19] A pioneering technology involves the hydrolase-catalyzed kinetic resolution (KR) of racemic amines (Scheme 1a), a reaction that is now well-established on an industrial scale.[20] Subsequently, the groundbreaking efforts by the group led by Turner introduced the deracemization of racemic amines as a viable route (Scheme 1b),[21] which, in comparison to the KR approach, is more atom-efficient. Besides, other elegant methods include Pictet−Spenglerase-catalyzed Pictet−Spengler cyclization (Scheme 1c),[22,23] cytochrome P450-catalyzed direct C−H amination (Scheme 1d),[24,25] and ammonia lyase-catalyzed hydroamination of α,β-unsaturated acids (Scheme 1c).[26,27] In addition, transaminase-catalyzed ARA-type transformations have also garnered attention over the past decade,[28] which, however, face significant challenges with pronounced substrate/product-inhibition and equilibrium displacement.[29] More recently, imine reductases (IREDs),[30−34] reductive aminases (RedAms),[35−39] and amine dehydrogenases (AmDHs)[40−49] have become the avant-garde in enzymatic ARA (Scheme 1f).

Despite over a decade of intensive research on enzymatic ARA reactions, merely a few of these reactions have transitioned to industrial application,[31,50−52] and/or met specific performance benchmarks concerning product concentrations and catalyst utilization (Table S1).[53−55] Presently, the performance of the enzymes catalyzing ARA confine them to

Received: September 26, 2024
Revised: November 26, 2024
Accepted: December 2, 2024

https://doi.org/10.1021/acscatal.4c05904
ACS Catal. 2025, 15, 34−43

Scheme 1. Biocatalytic Strategies for Chiral Amine Synthesis

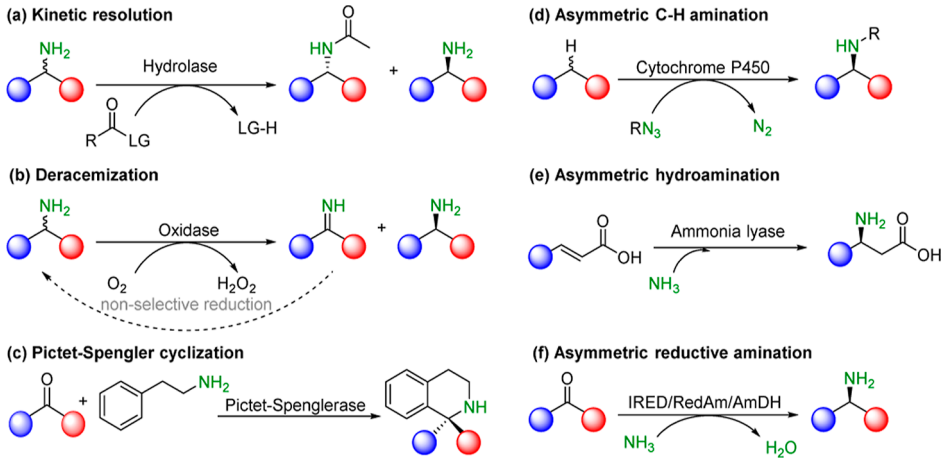

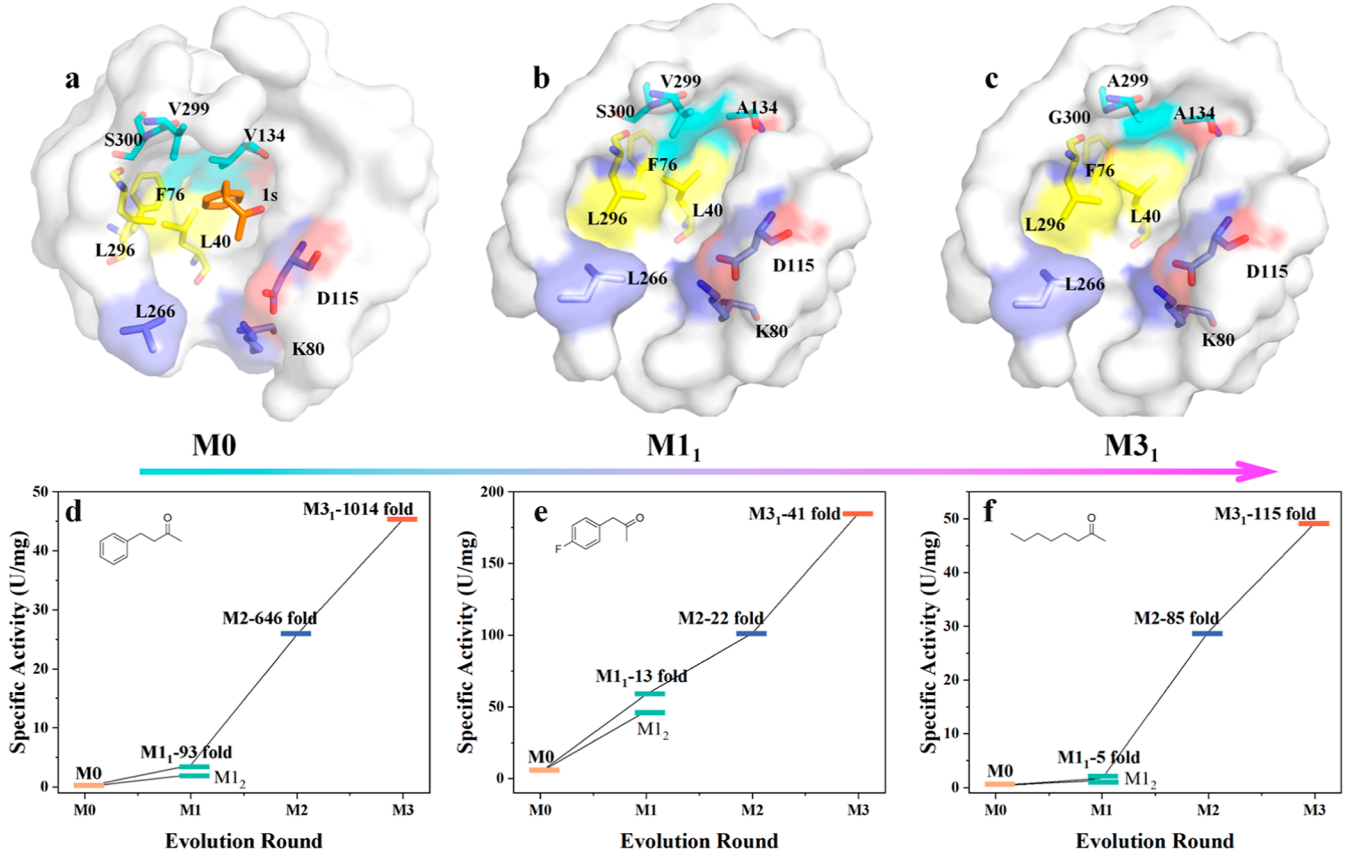

Figure 1. *Cal*AmDH variants obtained. (a) Structural model of M0. Mutation sites distribution on the structural model of $M1_1$ (b) and $M3_1$. (c) Evolution route of the starting enzyme M0, and the *Cal*AmDH mutants toward substrates **1s** (d), **19s** (e) and **37s** (f).

the high-value pharmaceutical domain (Table S2). To broaden the applicability of biocatalytic ARA to encompass larger volume chemicals and thereby significantly enhance its impact on the environmental footprint of the chemical industry, substantial enhancements in the performance of biocatalytic ARA are imperative.

Directed evolution, where mutant libraries are tested against increasing reagent concentrations, has predominantly been the strategy of choice to achieve industrial relevance. Although great process has been made in engineering of AmDHs, the ARA of bulky (especially aryl-substituted) ketones remains highly challenging, particularly at elevated reagent concentrations. An alternative strategy is bioprocess development involving reaction media and reactor design. Interestingly, while this approach has been demonstrated for various enzyme classes, successful examples for ARA-catalyzing biocatalysts are scarce.

In this context, we engineered an AmDH with high activity and substrate scope toward bulky ketones, and achieved the scale-up of this bioprocess in a fatty acid-containing aqueous buffer system. Recently, Pushpanath et al. introduced two mutations (K67S/N266L) into a phenylalanine dehydrogenase (*Cal*PheDH) from the thermophilic alkaliphilic bacterium *Caldalkalibacillus thermarum*, transforming it to an amine

https://doi.org/10.1021/acscatal.4c05904
ACS Catal. 2025, 15, 34−43

Scheme 2. Substrate Scope of the M3$_1$-Catalysed Reductive Amination[a]

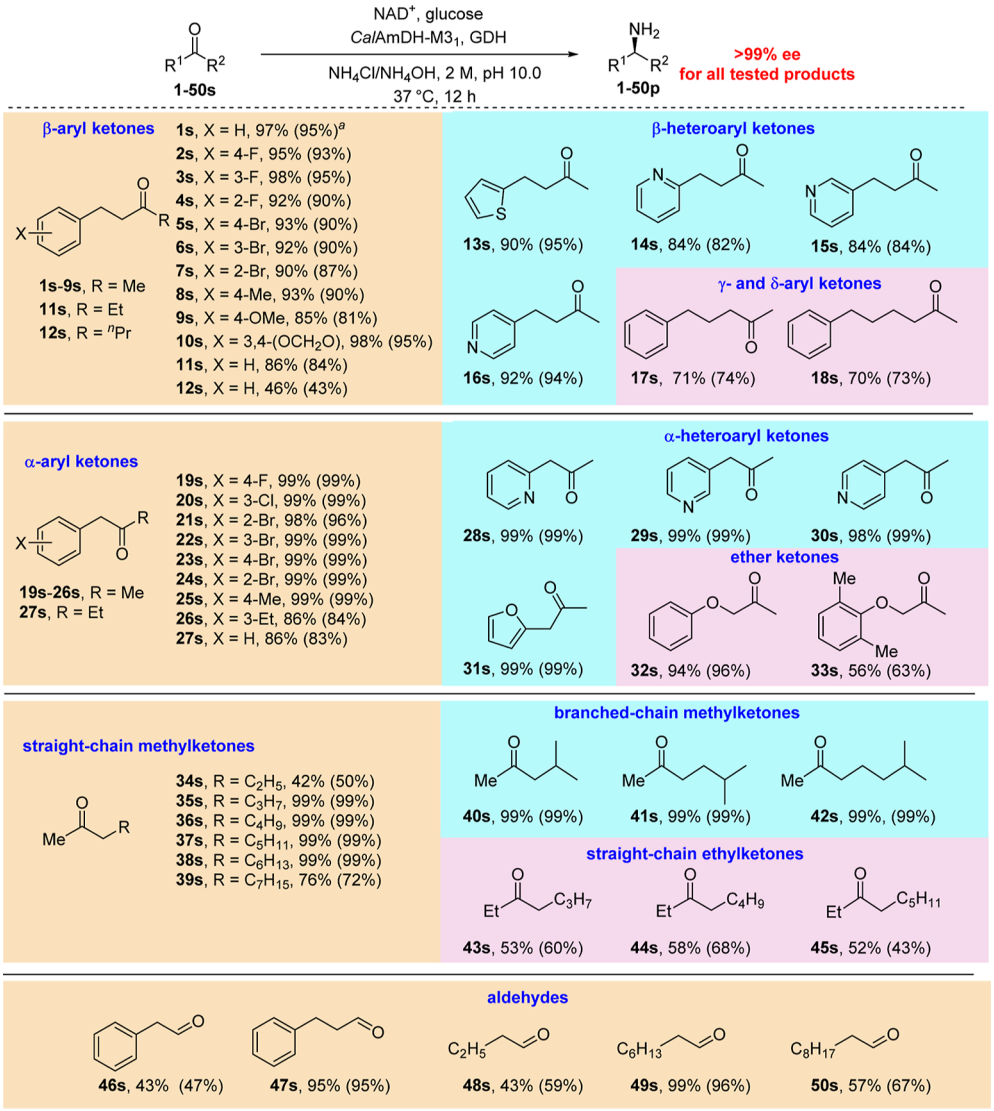

[a]Standard reaction conditions for 100 mM scale: substrate (0.5 mmol), glucose (1.2 equiv), NAD$^+$ (0.05% equiv), purified M3$_1$ (75 μg) and GDH (75 μg) in 5.0 mL buffer (NH$_4$Cl/NH$_4$OH, 2 M, pH 10.0) at 37 °C; for 1.0 M scale, substrate (5 mmol), M3$_1$ (lyophilized cell, 20 mg) and GDH (lyophilized cell, 20 mg) in buffer-oleic acid (4:1, v/v) system with other conditions unchanged. The ee values are based on chiral gas chromatography (GC) analysis after the derivatization of the products. GC conversions (results for 1.0 M scale reaction in parentheses).

dehydrogenase (*Cal*AmDH), which exhibited high thermostability but suffered from low activity and narrow substrate scope.[56] To overcome the shortcomings of the variant *Cal*AmDH (K67S/N266L), we chose it as the starting point (for the sake of clarity, referred to, in this work, as *Cal*AmDH-M0) for semirational enzyme design in this study, yielding *Cal*AmDH variants with significantly enhanced substrate range and catalytic efficiency. During process development, we discovered an unexpected activating and stabilizing influence of fatty acids on *Cal*AmDH, which stabilize a flexible loop region on the enzyme's surface. This finding led us to engineer *Cal*AmDH variants with improved activity. We also validated the potential for chemoenzymatic processes, extending the substrate range from carbonyl groups to simple aryl halides, alkenes, and alkynes. Ultimately, we report kilogram-scale syntheses predicated on advanced enzyme- and reaction-engineering strategies.

RESULTS AND DISCUSSION

Protein Engineering to Improve Enzymatic Performance. The initial variant, *Cal*AmDH-M0, demonstrated minimal activity (in the milliunits per milligram range) toward the targeted ketone substrates (Figure 1d–f). We posited that this could be due to suboptimal binding of the non-native ketone starting materials. To investigate this, we modeled benzylacetone (**1s**) into the active site of M0 (Figure 1a), where **1s** was positioned in a tight hydrophobic pocket, aligning its carbonyl oxygen atom at distances of 8.3 and 5.4 Å from the catalytically significant residues K80–NH$_2$ and D115-COOH, respectively, and situating the carbonyl carbon atom 6.1 Å away from the NADH-C4 (Figure S2). We hypothesized that the bulky amino acids L40, F76, V134, L296, and V299 might contribute to this nonideal binding (Figure S3), leading us to replace them with smaller residues such as alanine and glycine.

https://doi.org/10.1021/acscatal.4c05904
ACS Catal. 2025, 15, 34–43

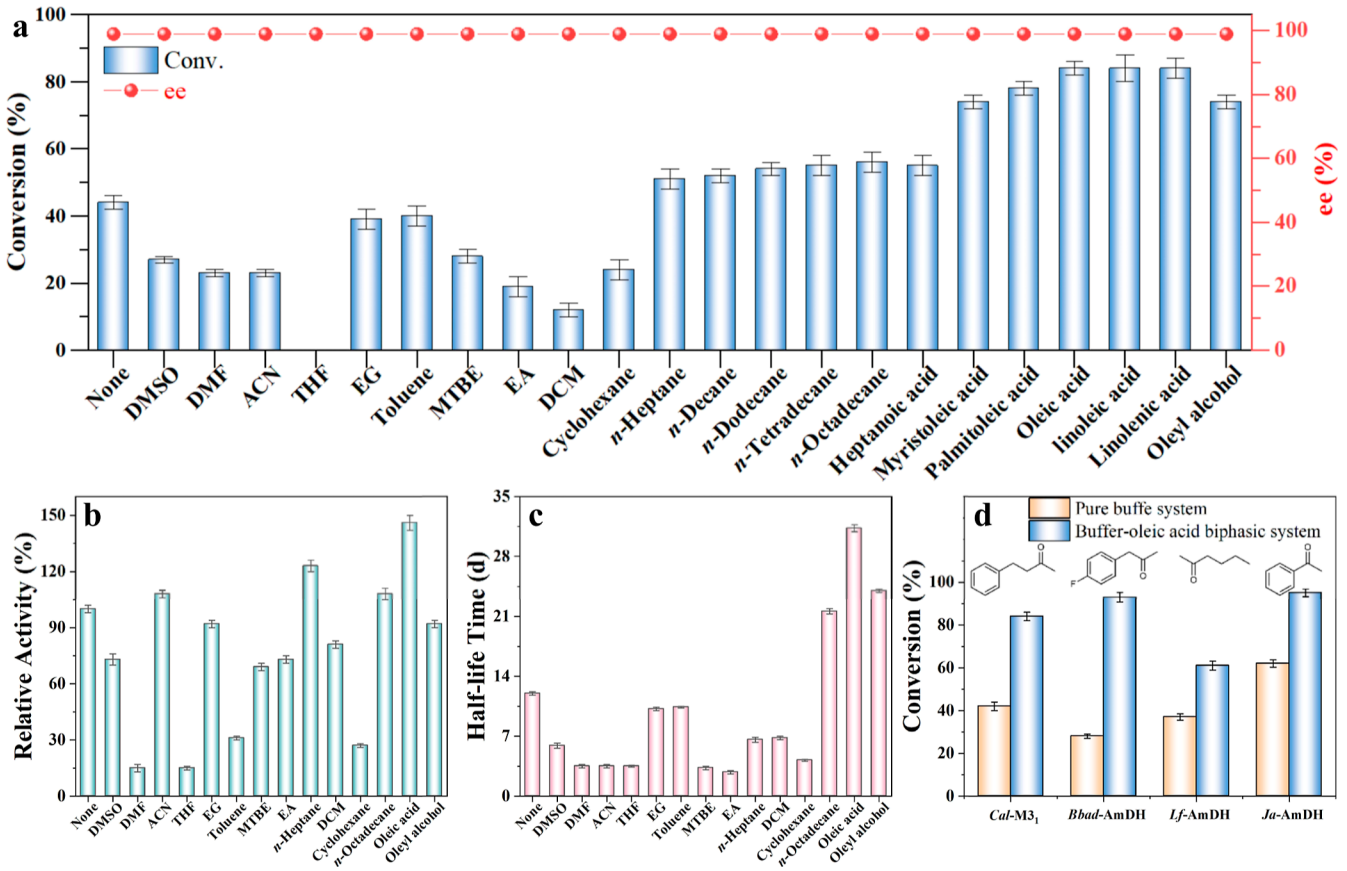

Figure 2. (a) Effect of organic solvents on enzyme performance. (b) Relative activity of $M3_1$ based on the linear approximation of reaction curves at substrate conversions ≤10% (initial rates). (c) Half-life time ($t_{1/2}$) of $M3_1$ after incubation in 20 vol% organic-aqueous biphasic systems. (d) AmDH-catalyzed ARA in pure buffer and buffer-oleic acid biphasic system.

Contrary to our expectations, modifications at positions 40, 76, and 296 led to a further decline in activity. However, variants V134A ($M1_1$) and V299A ($M1_2$) exhibited significant enhancements in activity toward **1s**, with 93-fold and 42-fold increases, respectively, compared to M0 (Figure 1d and Table S3). Similarly, these modifications notably amplified the activity toward model compounds **19s** and **37s** (Figure 1e,f). This improvement might be attributed to the expanded surface area and volume of the active sites in $M1_1$ and $M1_2$ (Table S4), potentially facilitating the formation of a productive transition state. Supporting this notion, both molecular docking (with calculated binding energies, Figure S4 and Table S5) and kinetic analyses (showing up to 95-fold increases in k_{cat}) corroborate our hypothesis. Combining the mutations from $M1_1$ and $M1_2$ to create mutant M2 led to a synergistic enhancement in catalytic activity for substrates **1s** (Figures 1d and S5 and Table S6) and **37s** (Figures 1f and S6 and Table S7). For substrate **19s**, the mutant M2 only led to a moderate enhancement in catalytic activity, which is due to that the k_{cat} values of $M1_1$ and $M1_2$ for **19s** were already higher than that of substrates **1s** and **37s**, achieving 54.0 and 44.8 s^{-1}, respectively (Figures 1e and S7 and Table S8). This enhancement can primarily be attributed to an increased k_{cat}, while the affinity of M2 for **1s** remained largely unchanged (Table S6). The introduction of an additional mutation, replacing hydrophilic S300 with glycine (V134A/V299A/S300G, $M3_1$), further augmented the enzyme's activity (Figure 1d–f). $M3_1$ also exhibited slight improvements in thermal and pH stability compared to M0. For example, at 50 °C and pH 10, $M3_1$ demonstrated half-lives ($t_{1/2}$) of 168 and 228 h, respectively, compared to 132 and 192 h for M0 (Figures S8–S11).

Subsequent experiments explored the substrate (100 mM) scope of $M3_1$ (Scheme 2), in which glucose dehydrogenase (GDH) was used for cofactor regeneration. While M0 showed no detectable conversion for substrates **1s**–**18s**, $M3_1$ achieved over 80% conversion for all tested β-(hetero)aryl ketones (**1s**–**16s**) except the propyl-bearing ketone **12s** (46%) under the same conditions. Conversions for the bulkier ketones **17s** (71%) and **18s** (70%) were lower. The aromatic ring substitution pattern had minimal impact on the conversion rates. The optical purity of the (*R*)-amine products was consistently greater than 99% enantiomeric excess (ee), with **1s** and **10s** being precursors for the antihypertensive drugs dilevalol and medroxalol.

For ketones **19s**–**33s**, $M3_1$ showed a specific activity significantly higher than M0, converting all α-(hetero)aryl ketones (**19s**–**31s**) to their corresponding 1-arylpropan-2-amines with greater than 98% conversion and greater than 99% ee, except the bulkier **26s** (86%). $M3_1$ was also effective with ether ketones **32s** and **33s**, and despite **33s**′ steric hindrance, its amination product (**33p**, i.e., mexiletine, an antiarrhythmic drug) was obtained in 56% conversion and greater than 99% ee.

While M0 exhibited minimal activity with aliphatic methylketones (**37s**–**42s**), $M3_1$ displayed significantly higher activity, with the conversion rates varying based on the alkyl chain length. Moreover, $M3_1$ efficiently converted more challenging ethyl ketones (**43s**–**45s**) with high enantioselec-

https://doi.org/10.1021/acscatal.4c05904
ACS Catal. 2025, 15, 34–43

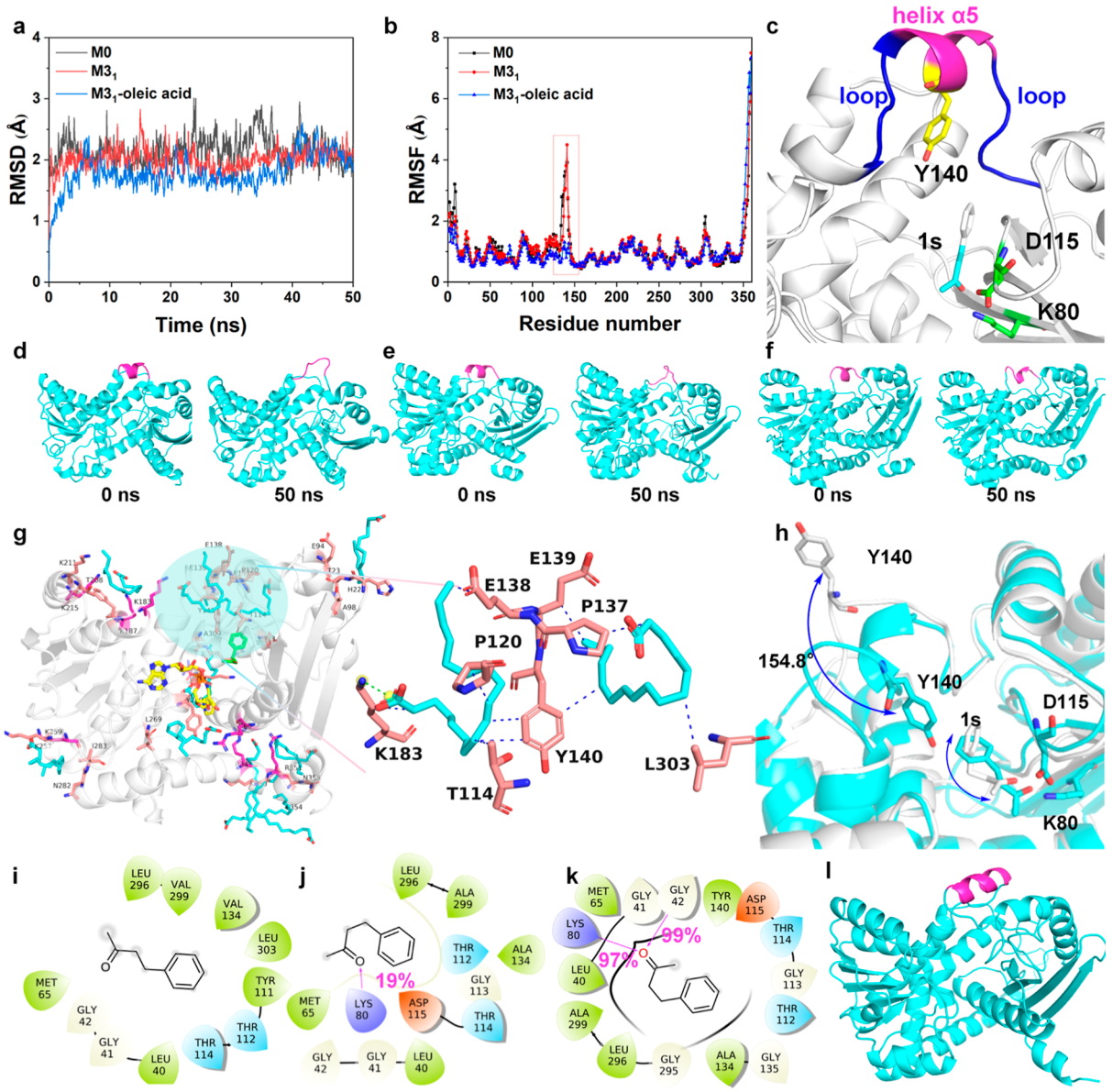

Figure 3. Variation of RMSD (a) and RMSF (b). (c) Cartoon models of the loop-α5-loop region. Snapshots of M0 (d) and M3$_1$ (e) in buffer solution, and of M3$_1$ in oleic acid-buffer solution (f). (g) Spatial distribution of oleic acid (shown in blue) on M3$_1$ within 4 Å in the MD simulations (left), and the interaction between oleic acid and α-helix 5 (right). (h) The direction of Y140 in oleic acid-buffer (blue) and pure buffer (gray) systems. Arrows indicate the flipping angle of Y140 and the shifting of substrates, respectively. The binding modes of **1s** to M0 (i) and of **1s** to M3$_1$ in the absence (j) and presence (k) of oleic acid (hydrophobic amino acids are represented by green water droplets, glycine by light-yellow water droplets, alkaline lysine by blue water droplets, and acidic amino acids by red water droplets). (l) Snapshots of M4 in buffer solution.

tivity. These products include sympathomimetic stimulants.[16] M3$_1$ also catalyzed the amination of aldehydes (**46s**−**50s**), with the conversion efficiency influenced by the steric demands of the substrates.

However, arylketones (such as the 4 examples shown in Figure S12) were somewhat sluggish substrates, which may be due to the existence of resonance and field effects derived from the phenyl ring, yielding a maximally 47% conversion under the reaction conditions chosen. The low reactivity of arylketones was also found by Mutti and co-workers.[58]

Unexpected Influence of Fatty Acids on *Cal*AmDH. Despite the improved performance of M3$_1$, only 45% conversion was achieved under 500 mM substrate (**1s**) concentration (Figure S13). In anticipation of the preparative application of M3$_1$, we explored various cosolvents to facilitate relevant reactant concentrations (Figure 2a).[57] Water-soluble cosolvents hindered the M3$_1$-catalyzed ARA of **1s**, whereas most hydrophobic cosolvents slightly enhanced the reaction compared to its absence. A similar phenomenon was also found by Au and co-workers.[59] Notably, the conversion of **1s** nearly doubled in the presence of fatty acids. In particular, oleic acid not only augmented M3$_1$'s activity (Figure 2b) but also substantially bolstered its robustness (Figure 2c). Notably, the oleic acid-induced conversion improvement for other AmDHs toward their respective substrates was also found (Figure 2d), including the enzymes from *Bacillus badius* (*Bbad*-AmDH[41]), *Lysinibacillus fusiformis* (*Lf*-AmDH[44]) and *Jeotgalicoccus aerolatus* (*Ja*-AmDH[46]), demonstrating the versatility of this approach.

https://doi.org/10.1021/acscatal.4c05904
ACS Catal. 2025, 15, 34−43

Scheme 3. Chemoenzymatic Synthesis of Chiral Pharmaceutically Relevant Amines

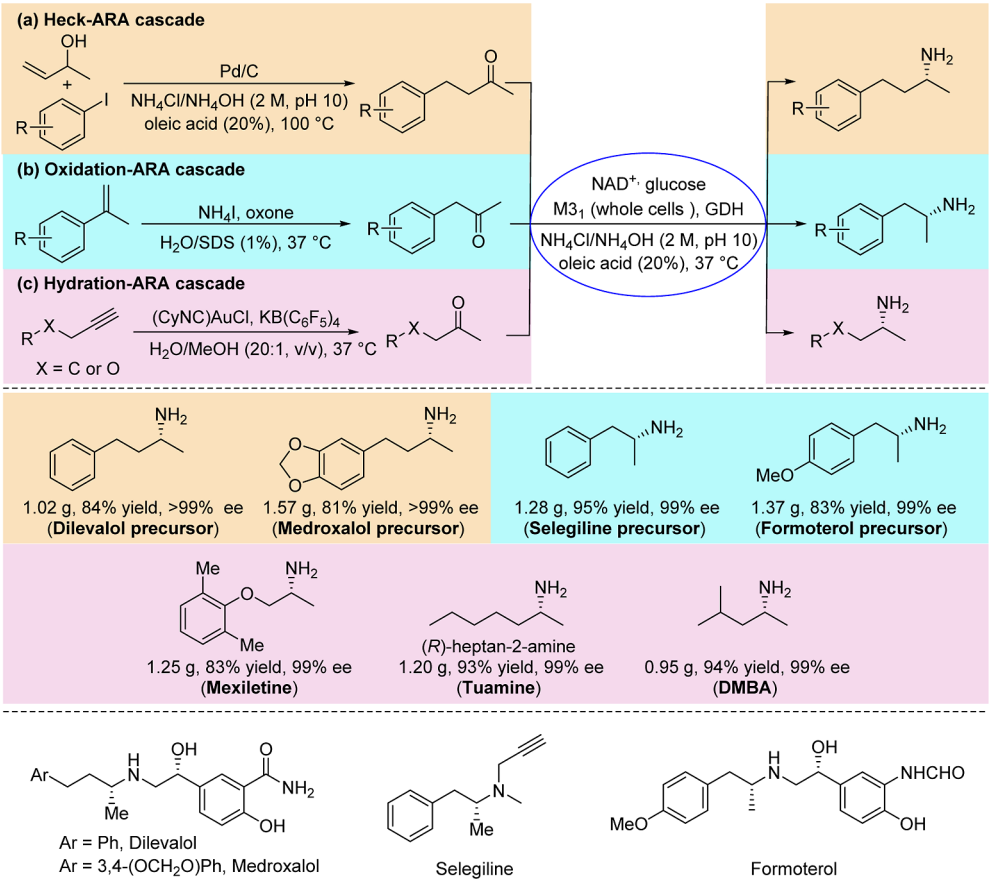

To elucidate the unexpected activating and stabilizing impact of fatty acids on $M3_1$, we conducted molecular dynamics (MD) simulations. The root-mean-square deviations (RMSD, Figure 3a) for M0, $M3_1$, and $M3_1$in the presence of oleic acid stabilized after approximately 10 ns, indicating no significant impact on the structural integrity of the enzyme. Similarly, the enzyme's secondary structure and amino acid residue interactions remained largely unchanged (Figures S14 and S15). However, the root-mean-square fluctuation (RMSF, Figure 3b) revealed a significant effect of oleic acid. In its absence, helix α5 (P137−N143) exhibited considerable flexibility (Figure 3c), eventually transitioning into a loop (Figures 3d,e and S16), a shift not observed with oleic acid present (Figure 3f). As shown in Figures 3g and S17, the presence of the carboxyl group gives oleic acid a completely different distribution position on the protein surface compared to *n*-octadecane. In particular, two oleic acid molecules are distributed in the α5 region and interact strongly with the α5 residues through hydrophobic interactions and salt bridges, blocking the helix-to-loop transition and thus stabilizing the enzyme conformation (Figure S18). In contrast, no enzyme stabilization effect was found in the case of *n*-octadecane molecules due to their absence in this region. In addition, the amphiphilic oleic acid can form micelles, thereby solubilizing the substrate and facilitating mass transfer, which is not possible with *n*-octadecane. Therefore, the carboxyl group of oleic acid plays an important role in improving enzymatic performance.

The significance of the helix-to-loop transition is underscored by examining Y140 (Figure 3h). In the helix state, Y140 forms close contacts (within hydrogen-bonding distance to K80 and G42) and is near the nicotinamide cofactor (Figure S19), facilitating substrate interaction. Conversely, in the loop state, Y140 points outward, disrupting these interactions. M0 did not exhibit this hydrogen bonding (Figure 3i), and it was only partially present in $M3_1$ (18% hydrogen bonding occupancy, Figure 3j). Oleic acid significantly enhanced these interactions (97% and 99% occupancy with K80 and G42, respectively, Figure 3k), explaining the observed rate acceleration. Additionally, oleic acid decreased the solvent-accessible surface area (SASA, Figure S20), enhancing interior packing interactions and potentially contributing to $M3_1$'s increased stability.

To experimentally confirm the important role of the α5 region, a helix engineering was performed by elongating the α5 fragment. As shown in Figure 3l, a α5-elongated new mutant (M4) was obtained by introducing 7 additional amino acids (PEEYGGN), which, as expected, exhibited further improvement in activity, stability, and kinetic parameters compared to $M3_1$ (Figures S10−S11 and Tables S6−S8). These findings not only underscored the significant impact of mutations distant from the active site on enzymatic performance, but also provided evidence that oleic acid, beyond serving as reaction media, can modulate enzyme's catalytic conformation, as directed evolution did. Notably, despite the further improved activity of AmDH-M4, it suffered from low soluble protein expression due to the partial formation of inclusion bodies, making its scale-up application problematic.

Equipped with $M3_1$ and optimized reaction conditions, we executed a semipreparative synthesis of (*R*)-4-phenylbutan-2-

https://doi.org/10.1021/acscatal.4c05904
ACS Catal. 2025, 15, 34−43

amine (**1p**) from **1s** (0.5 M). Employing a mere 20 mg × L^{-1} of purified $M3_1$ and 0.25 mM of NAD^+ in a biphasic system comprising buffer and oleic acid (4:1, v/v) at 37 °C for 12 h, we achieved a 95% yield and >99% ee (Figure S21). This equates to a total turnover number for $M3_1$ of 1,020,000 ($mol_{1p} \times mol_{M3_1}^{-1}$, translating to a product to biocatalyst ratio of 3540 g × g^{-1}) and an average turnover frequency of 23.6 s^{-1} over the 12 h period. The yield escalated to >99% when using lyophilized whole cells at a concentration of 4 g × L^{-1} (Figure S22), and the amount of oleic acid can be reduced to 8% (v/v) with 90% conversion (Figure S23). Consequently, the substrate concentration for all previously tested substrates could be increased to 1.0 M without any noticeable impact on conversions or enantioselectivities.

A kilogram-scale demonstration was conducted in a 10 L reactor using **1s** as a model substrate (refer to Supporting Information Methods, Figure S24). Traces of unreacted substrate were eliminated via extraction with ethyl acetate in acidic conditions, followed by a second extraction under basic conditions. Without any additional purification steps, 1.01 kg of the amine product (*R*)-**1p** was isolated (85% yield) with >99.9% ee. The total impurities remained below the gas chromatography detection threshold (<0.15%), satisfying the criteria for Good Manufacturing Practice (GMP) in active pharmaceutical ingredient (API) synthesis.

Constructing Chemoenzymatic Cascades to Expand the Feedstock Scope. Given the instability, costliness, or difficulty in obtaining certain ketone substrates, the utilization of cost-effective and readily accessible ketone precursors like olefins, alkynes, or alcohols is deemed advantageous. Toward this aim, three chemoenzymatic cascades were developed by amalgamating $M3_1$ with Pd-catalyzed Heck reaction of allylic alcohols,[60] hypoiodite-catalyzed anti-Markovnikov oxidation of alkenes,[61] and Au-catalyzed hydration of alkynes.[62]

In the Heck-ARA cascade, both processes were executed in the previously delineated buffer-oleic acid biphasic system. Owing to the Heck reaction's requirement for elevated temperatures (100 °C), it was carried out sans the biocatalyst. Post completion, the heterogeneous catalyst was recuperated, and the biocatalyst was incorporated for the ARA reaction at 37 °C. This one-pot sequential cascade facilitated the generation of chiral precursors for dilevalol and medroxalol from allyl alcohol and aryl halides (Scheme 3a).

For the subsequent cascades, the chemical catalysts displayed incompatibility with oleic acid, necessitating its addition after the chemical transformation and catalyst recycling, alongside the biocatalyst. The oxidation-ARA cascade enabled the asymmetric synthesis of amphetamine, precursors for formoterol, from olefins (Scheme 3b). Meanwhile, the hydration-ARA cascade produced mexiletine, heptan-2-amine (tuamine), and 1,3-dimethylbutylamine (DMBA) from alkynes (Scheme 3c). Conducted on a gram scale, these chemoenzeymatic cascades showcased over 80% overall yield and greater than 99.9% ee, highlighting their practical application in synthesizing pharmaceutically relevant amines.

CONCLUSION

In conclusion, the application of molecular docking and dynamic simulations for the enhancement of a thermostable AmDH's activity has proven to be a successful strategy in engineering catalysts that are both highly active and stable. Our findings underscore the significance of the often-overlooked loop regions in enzymes, highlighting their importance in catalysis. The product yields and catalyst efficiencies achieved with the engineered AmDH mutants suggest their potential applicability in the synthesis of commodity and even bulk chemicals. Thus, we demonstrate a pathway to liberate biocatalytic asymmetric reductive amination (ARA) from the confines of pharmaceutical niches. To date, however, biocatalytic reactions have been predominantly confined to this sector due to the insufficient efficiency of enzymes for the production of larger-scale (and more cost-effective) products.

The modest production volumes within the pharmaceutical sector constrain the potential of biocatalysis to significantly enhance environmental sustainability. We are convinced that this contribution adds a series of thought-provoking insights aimed at transcending this limitation, positioning biocatalysis as a transformative technology for the chemical industry.

Methods. *Enzyme Activity Assay.* The activities of AmDHs were measured by monitoring the change in the absorbance of NADH at 340 nm using a SpectraMax190 spectrophotometer (Molecular Devices, USA). The activity assay was conducted in a 1 mL reaction mixture comprising NH_4Cl/NH_4OH buffer (2.0 M, pH 10.0), 1 mM NADH, 50 mM substrate, and 15 μg/mL of purified enzyme, at 37 °C for a duration of 1.0 min. One unit of activity was defined as the amount of enzyme that catalyzes the conversion of 1 μmol of substrate per minute.

Enzymatic ARA. Substrate (5.0 mmol), glucose (1.2 equiv), NAD^+ (0.05% equiv), lyophilized whole cells of $M3_1$ (20.0 mg) and lyophilized whole cells of GDH (20.0 mg) in 5.0 mL buffer (NH_4Cl/NH_4OH, 2.0 M, pH 10.0)-oleic acid (4:1, v/v) were added to a 25 mL round-bottom flask. The mixture was stirred at 37 °C for 12 h. After the reaction was completed, the reaction solution was extracted with Et_2O (5 mL × 3). The organic phase was dried using anhydrous Na_2SO_4, and concentrated in vacuo to obtain the crude products. The products were purified by column chromatography using dichloromethane and methanol (10:1, v/v) as eluent.

ASSOCIATED CONTENT

Supporting Information

The Supporting Information is available free of charge at https://pubs.acs.org/doi/10.1021/acscatal.4c05904.

Materials and methods, optimization details, general catalytic procedure, figures, tables and analytical data (PDF)

AUTHOR INFORMATION

Corresponding Authors

Yunting Liu − *School of Chemical Engineering and Technology, Hebei University of Technology, Tianjin 300401, China;* orcid.org/0000-0003-3799-0362; Email: ytliu@hebut.edu.cn

Yanjun Jiang − *School of Chemical Engineering and Technology, Hebei University of Technology, Tianjin 300401, China;* orcid.org/0000-0003-1470-2102; Email: yanjunjiang@hebut.edu.cn

Authors

Weixi Kong − *School of Chemical Engineering and Technology, Hebei University of Technology, Tianjin 300401, China; Department of Electrical Engineering, Hebei*

Vocational University of Technology and Engineering, Xingtai 054000, China

Jiawang Zhang − *School of Chemical Engineering and Technology, Hebei University of Technology, Tianjin 300401, China*

Liya Zhou − *School of Chemical Engineering and Technology, Hebei University of Technology, Tianjin 300401, China*

Guanhua Liu − *School of Chemical Engineering and Technology, Hebei University of Technology, Tianjin 300401, China;* orcid.org/0000-0002-0824-9738

Ying He − *School of Chemical Engineering and Technology, Hebei University of Technology, Tianjin 300401, China;* orcid.org/0000-0002-8857-3545

Li Ma − *School of Chemical Engineering and Technology, Hebei University of Technology, Tianjin 300401, China*

Frank Hollmann − *Department of Biotechnology, Delft University of Technology, Delft 2629 HZ, The Netherlands;* orcid.org/0000-0003-4821-756X

Lihui Wang − *School of Department Biochemical Engineering, Tianjin Modern Vocational Technology College, Tianjin 300130, China*

Complete contact information is available at: https://pubs.acs.org/10.1021/acscatal.4c05904

Author Contributions

The manuscript was written through contributions of all authors. All authors have given approval to the final version of the manuscript.

Notes

The authors declare no competing financial interest.

■ ACKNOWLEDGMENTS

This work was supported by the National Key Research and Development Program of China (2023YFA0914500), the National Natural Science Foundation of China (nos. 22378096, 22308083 and 22178083), the Natural Science Foundation of Hebei Province (nos. B2023202014 and B2022202014), Tianjin Science and technology planning project (24YDTPJC00990) and the S&T program of Hebei (nos. 21372805D and 21372804D). Funded by the European Union (ERC, PeroxyZyme, no 101054658). Views and opinions expressed are however those of the authors only and do not necessarily reflect those of the European Union or the European Research Council. Neither the European Union nor the granting authority can be held responsible for them.

■ REFERENCES

(1) *Methodologies in Amine Synthesis: Challenges and Applications*; Ricci, A.; Bernardi, L., Eds.; Wiley, 2021; p 480.

(2) *Chiral Amine Synthesis: Methods, Developments and Applications*; Nugent, T. C., Ed.; Wiley, 2010; p 7841.

(3) Lindqvist, M.; Borre, K.; Axenov, K.; Kótai, B.; Nieger, M.; Leskelä, M.; Pápai, I.; Repo, T. Chiral Molecular Tweezers: Synthesis and Reactivity in Asymmetric Hydrogenation. *J. Am. Chem. Soc.* **2015**, *137* (12), 4038−4041.

(4) Xie, J.; Zhu, S.; Zhou, Q. Transition Metal-Catalyzed Enantioselective Hydrogenation of Enamines and Imines. *Chem. Rev.* **2011**, *111* (3), 1713−1760.

(5) Wang, J.; Li, Y.; Nie, W.; Chang, Z.; Yu, Z.; Zhao, Y.; Lu, X.; Fu, Y. Catalytic Asymmetric Reductive Hydroalkylation of Enamides and Enecarbamates to Chiral Aliphatic Amines. *Nat. Commun.* **2021**, *12* (1), 1313.

(6) Qian, D.; Bera, S.; Hu, X. Chiral Alkyl Amine Synthesis via Catalytic Enantioselective Hydroalkylation of Enecarbamates. *J. Am. Chem. Soc.* **2021**, *143* (4), 1959−1967.

(7) Wang, S.; Zhang, J.; Zhang, T.; Meng, H.; Chen, B.; Shu, W. Enantioselective Access to Chiral Aliphatic Amines and Alcohols via Ni-Catalyzed Hydroalkylations. *Nat. Commun.* **2021**, *12* (1), 2771.

(8) Chen, J.; Fang, J.; Du, X.; Zhang, J.; Bian, J.; Wang, F.; Luan, C.; Liu, W.; Liu, J.; Dong, X.; Li, Z.; Gu, Q.; Dong, Z.; Liu, X. Enantioconvergent Cu-Catalysed N-alkylation of Aliphatic Amines. *Nature* **2023**, *618* (7964), 294−300.

(9) Davies, H. M. L.; Manning, J. R. Catalytic C−H Functionalization by Metal Carbenoid and Nitrenoid Insertion. *Nature* **2008**, *451* (7177), 417−424.

(10) Park, Y.; Kim, Y.; Chang, S. Transition Metal-Catalyzed C-H Amination: Scope, Mechanism, and Applications. *Chem. Rev.* **2017**, *117* (13), 9247−9301.

(11) Li, M.; Yu, J.; Li, Y.; Zhu, S.; Zhou, Q. Highly Enantioselective Carbene Insertion into N−H Bonds of Aliphatic Amines. *Science* **2019**, *366* (6468), 990−994.

(12) Pirnot, M. T.; Wang, Y. M.; Buchwald, S. L. Copper Hydride Catalyzed Hydroamination of Alkenes and Alkynes. *Angew. Chem., Int. Ed.* **2016**, *55* (1), 48−57.

(13) Qin, T.; Lv, G.; Meng, Q.; Zhang, G.; Xiong, T.; Zhang, Q. Cobalt-Catalyzed Radical Hydroamination of Alkenes with N-Fluorobenzenesulfonimides. *Angew. Chem., Int. Ed.* **2021**, *60* (49), 25949−25957.

(14) Zhu, S.; Niljianskul, N.; Buchwald, S. L. Enantio- and Regioselective CuH-Catalyzed Hydroamination of Alkenes. *J. Am. Chem. Soc.* **2013**, *135* (42), 15746−15749.

(15) Wu, Z.; Wang, W.; Guo, H.; Gao, G.; Huang, H.; Chang, M. Iridium-Catalyzed Direct Asymmetric Reductive Amination Utilizing Primary Alkyl Amines as the N-Sources. *Nat. Commun.* **2022**, *13* (1), 3344.

(16) Hu, L.; Zhang, Y.; Zhang, Q.; Yin, Q.; Zhang, X. Ruthenium-Catalyzed Direct Asymmetric Reductive Amination of Diaryl and Sterically Hindered Ketones with Ammonium Salts and H_2. *Angew. Chem., Int. Ed.* **2020**, *59* (13), 5321−5325.

(17) Tan, X.; Gao, S.; Zeng, W.; Xin, S.; Yin, Q.; Zhang, X. Asymmetric Synthesis of Chiral Primary Amines by Ruthenium-Catalyzed Direct Reductive Amination of Alkyl Aryl Ketones with Ammonium Salts and Molecular H_2. *J. Am. Chem. Soc.* **2018**, *140* (6), 2024−2027.

(18) Gallardo-Donaire, J.; Hermsen, M.; Wysocki, J.; Ernst, M.; Rominger, F.; Trapp, O.; Hashmi, A.; Schäfer, A.; Comba, P.; Schaub, T. Direct Asymmetric Ruthenium-Catalyzed Reductive Amination of Alkyl−Aryl Ketones with Ammonia and Hydrogen. *J. Am. Chem. Soc.* **2018**, *140* (1), 355−361.

(19) Abdelraheem, E.; Damian, M.; Mutti, F. G. Biocatalytic Amine Synthesis. *Comprehensive Chirality*, 2nd ed., 2024; pp 210−304.

(20) Wu, S.; Snajdrova, R.; Moore, J. C.; Baldenius, K.; Bornscheuer, U. T. Biocatalysis: Enzymatic Synthesis for Industrial Applications. *Angew. Chem., Int. Ed.* **2021**, *60* (1), 88−119.

(21) Turner, N. J. Enantioselective Oxidation of C-O and C-N Bonds Using Oxidases. *Chem. Rev.* **2011**, *111* (7), 4073−4087.

(22) Maresh, J. J.; Giddings, L. A.; Friedrich, A.; Loris, E. A.; Panjikar, S.; Trout, B. L.; Stöckigt, J.; Peters, B.; O'Connor, S. E. Strictosidine Synthase: Mechanism of a Pictet−Spengler Catalyzing Enzyme. *J. Am. Chem. Soc.* **2008**, *130* (2), 710−723.

(23) Wu, F.; Zhu, H.; Sun, L.; Rajendran, C.; Wang, M.; Ren, X.; Panjikar, S.; Cherkasov, A.; Zou, H.; Stöckigt, J. Scaffold Tailoring by a Newly Detected Pictet−Spenglerase Activity of Strictosidine Synthase: From the Common Tryptoline Skeleton to the Rare Piperazino-Indole Framework. *J. Am. Chem. Soc.* **2012**, *134* (3), 1498−1500.

(24) Goldberg, N. W.; Knight, A. M.; Zhang, R. K.; Arnold, F. H. Nitrene Transfer Catalyzed by a Non-Heme Iron Enzyme and Enhanced by Non-Native Small-Molecule Ligands. *J. Am. Chem. Soc.* **2019**, *141* (50), 19585−19588.

(25) Prier, C. K.; Zhang, R. K.; Buller, A. R.; Brinkmann-Chen, S.; Arnold, F. H. Enantioselective, intermolecular benzylic C−H amination catalysed by an engineered iron-haem enzyme. *Nat. Chem.* **2017**, *9* (7), 629−634.
(26) Ahmed, S. T.; Parmeggiani, F.; Weise, N. J.; Flitsch, S. L.; Turner, N. J. Engineered Ammonia Lyases for the Production of Challenging Electron-Rich l-Phenylalanines. *ACS Catal.* **2018**, *8* (4), 3129−3132.
(27) Li, R.; Wijma, H. J.; Song, L.; Cui, Y.; Otzen, M.; Tian, Y. e.; Du, J.; Li, T.; Niu, D.; Chen, Y.; Feng, J.; Han, J.; Chen, H.; Tao, Y.; Janssen, D. B.; Wu, B. Computational Redesign of Enzymes for Regio- and Enantioselective Hydroamination. *Nat. Chem. Bio.* **2018**, *14* (7), 664−670.
(28) Ferrandi, E. E.; Monti, D. Amine Transaminases in Chiral Amines Synthesis: Recent Advances and Challenges. *World J. Microbiol. Biotechnol.* **2018**, *34* (1), 13.
(29) Kelly, S.; Pohle, S.; Wharry, S.; Mix, S.; Allen, C.; Moody, T.; Gilmore, B. F. J. C. R. Application of ω-Transaminases in the Pharmaceutical Industry. *Chem. Rev.* **2018**, *118* (1), 349−367.
(30) Marshall, J. R.; Yao, P.; Montgomery, S. L.; Finnigan, J. D.; Thorpe, T. W.; Palmer, R. B.; Mangas-Sanchez, J.; Duncan, R. A. M.; Heath, R. S.; Graham, K. M.; Cook, D. J.; Charnock, S. J.; Turner, N. J. Screening and Characterization of a Diverse Panel of Metagenomic Imine Reductases for Biocatalytic Reductive Amination. *Nat. Chem.* **2021**, *13* (2), 140−148.
(31) Schober, M.; MacDermaid, C.; Ollis, A. A.; Chang, S.; Khan, D.; Hosford, J.; Latham, J.; Ihnken, L. A. F.; Brown, M. J. B.; Fuerst, D.; Sanganee, M. J.; Roiban, G. D. Chiral Synthesis of LSD1 Inhibitor GSK2879552 Enabled by Directed Evolution of an Imine Reductase. *Nat. Catal.* **2019**, *2* (10), 909−915.
(32) Wetzl, D.; Gand, M.; Ross, A.; Müller, H.; Matzel, P.; Hanlon, S. P.; Müller, M.; Wirz, B.; Höhne, M.; Iding, H. Asymmetric Reductive Amination of Ketones Catalyzed by Imine Reductases. *ChemCatChem* **2016**, *8* (12), 2023−2026.
(33) Huber, T.; Schneider, L.; Präg, A.; Gerhardt, S.; Einsle, O.; Müller, M. Direct Reductive Amination of Ketones: Structure and Activity of *S*-Selective Imine Reductases from *Streptomyces*. *ChemCatChem* **2014**, *6* (8), 2248−2252.
(34) Chen, F.; He, X.; Zhu, X.; Zhang, Z.; Shen, X.; Chen, Q.; Xu, J.; Turner, N. J.; Zheng, G. Discovery of an Imine Reductase for Reductive Amination of Carbonyl Compounds with Sterically Challenging Amines. *J. Am. Chem. Soc.* **2023**, *145* (7), 4015−4025.
(35) Aleku, G. A.; France, S. P.; Man, H.; Mangas-Sanchez, J.; Montgomery, S. L.; Sharma, M.; Leipold, F.; Hussain, S.; Grogan, G.; Turner, N. J. A Reductive Aminase from Aspergillus Oryzae. *Nat. Chem.* **2017**, *9* (10), 961−969.
(36) Li, B.; Zhang, J.; Chen, F.; Chen, Q.; Xu, J.; Zheng, G. Direct Reductive Amination of Ketones with Amines by Reductive Aminases. *Green Synth. Catal.* **2021**, *2* (4), 345−349.
(37) González-Martínez, D.; Cuetos, A.; Sharma, M.; García-Ramos, M.; Lavandera, I.; Gotor-Fernández, V.; Grogan, G. Asymmetric Synthesis of Primary and Secondary β-Fluoro-arylamines using Reductive Aminases from Fungi. *ChemCatChem* **2020**, *12* (9), 2421−2425.
(38) Ducrot, L.; Bennett, M.; Grogan, G.; Vergne-Vaxelaire, C. NAD(P)H-Dependent Enzymes for Reductive Amination: Active Site Description and Carbonyl-Containing Compound Spectrum. *Adv. Synth. Catal.* **2020**, *363* (2), 328−351.
(39) Sharma, M.; Mangas-Sanchez, J.; France, S. P.; Aleku, G. A.; Montgomery, S. L.; Ramsden, J. I.; Turner, N. J.; Grogan, G. A Mechanism for Reductive Amination Catalyzed by Fungal Reductive Aminases. *ACS Catal.* **2018**, *8* (12), 11534−11541.
(40) Abrahamson, M. J.; Vázquez-Figueroa, E.; Woodall, N. B.; Moore, J. C.; Bommarius, A. S. Development of an Amine Dehydrogenase for Synthesis of Chiral Amines. *Angew. Chem., Int. Ed.* **2012**, *51* (16), 3969−3972.
(41) Abrahamson, M. J.; Wong, J. W.; Bommarius, A. S. The Evolution of an Amine Dehydrogenase Biocatalyst for the Asymmetric Production of Chiral Amines. *Adv. Synth. Catal.* **2013**, *355* (9), 1780−1786.
(42) Bommarius, B. R.; Schurmann, M.; Bommarius, A. S. A Novel Chimeric Amine Dehydrogenase Shows Altered Substrate Specificity Compared to its Parent Enzymes. *Chem. Commun.* **2014**, *50* (95), 14953−14955.
(43) Chen, F.; Zheng, G.; Liu, L.; Li, H.; Chen, Q.; Li, F.; Li, C.; Xu, J. Reshaping the Active Pocket of Amine Dehydrogenases for Asymmetric Synthesis of Bulky Aliphatic Amines. *ACS Catal.* **2018**, *8* (3), 2622−2628.
(44) Chen, F.; Cosgrove, S.; Birmingham, W.; Mangas-Sanchez, J.; Citoler, J.; Thompson, M. P.; Zheng, G.; Xu, J.; Turner, N. J. Enantioselective Synthesis of Chiral Vicinal Amino Alcohols Using Amine Dehydrogenases. *ACS Catal.* **2019**, *9* (12), 11813−11818.
(45) Tseliou, V.; Knaus, T.; Masman, M.; Corrado, M.; Mutti, F. Generation of Amine Dehydrogenases with Increased Catalytic Performance and Substrate Scope from ε-Deaminating L-Lysine Dehydrogenase. *Nat. Commun.* **2019**, *10* (1), 3717.
(46) Kong, W.; Liu, Y.; Huang, C.; Zhou, L.; Gao, J.; Turner, N. J.; Jiang, Y. Direct Asymmetric Reductive Amination of Alkyl (Hetero)-Aryl Ketones by an Engineered Amine Dehydrogenase. *Angew. Chem., Int. Ed.* **2022**, *61* (21), No. e202202264.
(47) Mayol, O.; Bastard, K.; Beloti, L.; Frese, A.; Turkenburg, J.; Petit, J.; Mariage, A.; Debard, A.; Pellouin, V.; Perret, A.; de Berardinis, V.; Zaparucha, A.; Grogan, G.; Vergne-Vaxelaire, C. A Family of Native Amine Dehydrogenases for the Asymmetric Reductive Amination of Ketones. *Nat. Catal.* **2019**, *2* (4), 324−333.
(48) Tseliou, V.; Masman, M. F.; Knaus, T.; Mutti, F. G. Current Status of Amine Dehydrogenases: From Active Site Architecture to Diverse Applications Across a Broad Substrate Spectrum. *ChemCatChem* **2024**, No. e202400469.
(49) Yin, X.; Gong, W.; Zeng, Y.; Qiu, H.; Liu, L.; Hollmann, F.; Chen, B. Substrate-Specific Evolution of Amine Dehydrogenases for Accessing Structurally Diverse Enantiopure (*R*)-β-Amino Alcohols. *ACS Catal.* **2024**, *14* (2), 837−845.
(50) Bornadel, A.; Bisagni, S.; Pushpanath, A.; Montgomery, S.; Turner, N. J.; Dominguez, B. Technical Considerations for Scale-up of Imine-Reductase-Catalyzed Reductive Amination: A Case Study. *Org. Process Res. Dev.* **2019**, *23* (6), 1262−1268.
(51) Savile, C. K.; Janey, J. M.; Mundorff, E. C.; Moore, J. C.; Tam, S.; Jarvis, W. R.; Colbeck, J. C.; Krebber, A.; Fleitz, F. J.; Brands, J.; Devine, P. N.; Huisman, G. W.; Hughes, G. J. Biocatalytic Asymmetric Synthesis of Chiral Amines from Ketones Applied to Sitagliptin Manufacture. *Science* **2010**, *329* (5989), 305−309.
(52) Kumar, R.; Karmilowicz, M. J.; Burke, D.; Burns, M. P.; Clark, L. A.; Connor, C. G.; Cordi, E.; Do, N. M.; Doyle, K. M.; Hoagland, S.; Lewis, C. A.; Mangan, D.; Martinez, C. A.; McInturff, E. L.; Meldrum, K.; Pearson, R.; Steflik, J.; Rane, A.; Weaver, J. Biocatalytic Reductive Amination from Discovery to Commercial Manufacturing Applied to Abrocitinib JAK1 Inhibitor. *Nat. Catal.* **2021**, *4* (9), 775−782.
(53) Madsen, J. Ø.; Woodley, J. M. Considerations for the Scale-up of in vitro Transaminase-Catalyzed Asymmetric Synthesis of Chiral Amines. *ChemCatChem* **2023**, *15* (13), No. e202300560.
(54) Tufvesson, P. R.; Lima-Ramos, J.; Nordblad, M.; Woodley, J. M. Guidelines and Cost Analysis for Catalyst Production in Biocatalytic Processes. *Org. Process Res. Dev.* **2011**, *15* (1), 266−274.
(55) Tufvesson, P.; Fu, W.; Jensen, J. S.; Woodley, J. M. Process Considerations for the Scale-up and Implementation of Biocatalysis. *Food Bioprod. Process.* **2010**, *88* (1), 3−11.
(56) Pushpanath, A.; Siirola, E.; Bornadel, A.; Woodlock, D.; Schell, U. Understanding and Overcoming the Limitations of Bacillus Badius and *Caldalkalibacillus Thermarum* Amine Dehydrogenases for Biocatalytic Reductive Amination. *ACS Catal.* **2017**, *7* (5), 3204−3209.
(57) Wubbolts, M. G.; FavreBulle, O.; Witholt, B. Biosynthesis of Synthons in Two-Liquid-Phase Media. *Biotechnol. Bioeng.* **1996**, *52* (2), 301−308.

(58) Knaus, T.; Bohmer, W.; Mutti, F. G. Amine Dehydrogenases: Efficient Biocatalysts for the Reductive Amination of Carbonyl Compounds. *Green Chem.* **2017**, *19* (2), 453−463.
(59) Au, S. K.; Bommarius, B. R.; Bommarius, A. S. Biphasic Reaction System Allows for Conversion of Hydrophobic Substrates by Amine Dehydrogenases. *ACS Catal.* **2014**, *4* (11), 4021−4026.
(60) Boffi, A.; Cacchi, S.; Ceci, P.; Cirilli, R.; Fabrizi, G.; Prastaro, A.; Niembro, S.; Shafir, A.; Vallribera, A. The Heck Reaction of Allylic Alcohols Catalyzed by Palladium Nanoparticles in Water: Chemo-enzymatic Synthesis of (*R*)-(−)-Rhododendrol. *ChemCatChem* **2011**, *3* (2), 347−353.
(61) Swamy, P.; Reddy, M. M.; Naresh, M.; Kumar, M. A.; Srujana, K.; Durgaiah, C.; Narender, N. Hypoiodite-Catalyzed Regioselective Oxidation of Alkenes: An Expeditious Access to Aldehydes in Aqueous Micellar Media. *Adv. Synth. Catal.* **2015**, *357* (6), 1125−1130.
(62) Xu, Y.; Hu, X.; Shao, J.; Yang, G.; Wu, Y.; Zhang, Z. Hydration of Alkynes at Room Temperature Catalyzed by Gold(i) Isocyanide Compounds. *Green Chem.* **2015**, *17* (1), 532−537.

https://doi.org/10.1021/acscatal.4c05904
ACS Catal. 2025, 15, 34−43